The Matrix Revisited

S. BREAKSPEAR, TREFOR EVANS, B. NOECKER AND C. POPESCU

KAO European Research Laboratories, KAO Germany GmbH, Darmstadt, Germany (S.B., B.N., C.P.)

TRI Princeton, Princeton, New Jersey, USA (T.E.)

Synopsis

Feughelman's two-phase model for keratin fibers provides a means for conceptualizing the properties and roles of differing protein structures within hair. Specifically, the crystalline α-helical keratin proteins that constitute the intermediate filaments/microfibrils are impenetrable to water, whereas the amorphous keratin within the surrounding matrix/keratin-associated protein is readily infiltrated. The presence of water solvates electrostatic bonding and progressively diminishes the contribution of the matrix protein through plasticization. In short, the wet-state mechanical properties of the fiber become dependent solely on the microfibrils, whereas in the dry state, the matrix also contributes to the structural integrity. In the hair care industry, there is a much higher tendency to perform hair testing in the wet state (e.g., wet-state instrumental combing, wet tensile testing, and even wet-state differential scanning calorimetry); however, such measurements contain no information about the amorphous matrix. Tensile experiments performed in the dry state show that the Young's modulus can be two to three times higher than in the wet state, so clearly, the matrix can have a sizable contribution to fiber properties. The negative effects of various chemical treatments are well documented in wet-state tensile experiments, but dry-state testing can present anomalies. In particular, it is common to see the dry-state modulus increase after such treatments. It is worth emphasizing that this overall rise in modulus occurs even though the microfibril contribution is diminished. This suggests an enhanced matrix contribution that, in some cases, can be very sizable. This article presents a review of the literature focusing on how the matrix structure is described, in an effort to understand the contribution of the matrix to fiber properties. These ideas are supplemented with the authors' experimental data to illustrate pertinent points and highlight some nontraditional outcomes and ideas.

BACKGROUND

Hair, the protective keratin fiber of mammal skin, is a focus for many researchers, because it offers hints into the world of biology and proteins and its unique composite architecture inspires material scientists. Its maintenance is also at the heart of a multibillion-dollar cosmetic industry.

Morphologically, hair can be described as a multicellular tissue consisting of several structural components: the cortex, made of spindle-like cortical cells; potentially a medulla, representing a core channel-like structure; and a cuticle layer that wraps the whole ensemble with sheets of rectangular cells. Each component plays a role in the overall properties of keratin fibers, with the cortex being primarily responsible for the mechanical attributes of strength and rigidity.

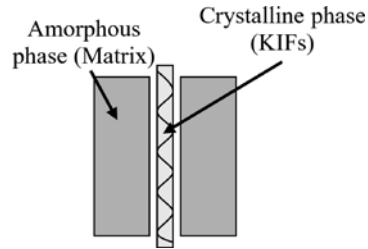Address all correspondence to Trefor Evans, tevans@triprinceton.org

Figure 1. Two-phase model of keratin fibers according to Feughelman's original model (1).

WHAT IS THE MATRIX?

More specifically, the cortex is a complex composite made of a number of components, the most important of which are crystalline keratin intermediate filaments (KIFs), amorphous keratin-associated proteins (KAPs), a medulla, a lipid-like cellular membrane complex (CMC), and melanin.

The term "matrix," as it is used today, was introduced by Feughelman (1) as part of his proposed two-phase (amorphous–crystalline) model of keratin fibers. That is, crystalline keratin rod structures pack within an amorphous keratin matrix (see Figure 1).

EXPERIMENTAL DETAILS

MECHANICAL TESTING

All tensile testing was performed on a Dia-Stron MTT600 miniature tensile tester (Dia-Stron Ltd., Andover, UK) that was housed in a benchtop environmental chamber. Test samples consisted of 30 mm hair fibers that were sandwiched between two brass ferrules using a crimping block. Conventional tensile testing was performed by stretching 50 replicate test fibers to their break point at a rate of 40 mm/min. Wet-state testing was performed by filling the sample slots in the testing carousel with deionized water. Unless otherwise stated, dry-state testing was performed at 60% relative humidity (RH). The data shown in Figure 2 were generated in this manner.

This article also shows data from an alternative approach to monitor the Young's modulus of fibers as a function of the relative humidity (e.g., see Figures 3A and 11). In this instance, all fibers were extended to 5% extension at a rate of 10 mm/min after equilibration at a specific humidity. After this process, the initial structure of all fibers could be regenerated by equilibration at elevated (90%) humidity for 4 h. The same fibers could then be equilibrated at a new humidity before being rerun in a similar experiment. In this way, Young's modulus results could be generated as a function of relative humidity without the need to prepare new samples each time.

TORSION TESTING

Torsional moduli were measured using a torsion pendulum approach that was described previously (2). In short, experiments were performed on a custom-built instrument with

which individual fibers were automatically and reproducibly induced into a twisting motion. The periodicity and dampening of this motion was then used to calculate mechanical parameters associated with this mode of deformation. The instrument was housed in a benchtop environmental chamber, and testing involved 30 replicate fibers per test condition.

DIFFERENTIAL SCANNING CALORIMETRY

Wet-state differential scanning calorimetry (DSC) investigations were performed on a PerkinElmer DSC 8500 instrument using pressure-resistant (25 bar) stainless steel large-volume capsules (PerkinElmer). The temperature was increased from 50 to 180°C at a heating rate of 10°C/min, while the chamber was being flushed with a nitrogen flow of 10 mL/min. Previously conditioned snippets of 5–6 mg from each sample were precisely weighed and placed in the stainless steel crucible. Then, 50 μL of distilled water (pH 6.7) was added, and the crucible was sealed and stored overnight.

Dry-state DSC measurements were performed on a Netzsch DSC 204 instrument using aluminum pans. The temperature was increased from 50 to 250°C at a heating rate of 10°C/min, while the chamber was being flushed with a nitrogen flow of 20 mL/min. Previously conditioned snippets of 5–6 mg from each sample were precisely weighed and placed in the aluminum crucible, which was covered with a lid. The lid was double pierced to allow product gases to evolve.

Calibration in all DSC experiments was performed using indium and palmitic acid, both of high purity. For each sample, three measurements were performed to ensure reproducibility of the data, and the peak temperature, T_p, and enthalpy, ΔH, of the endothermal effect were recorded.

ATOMIC FORCE MICROSCOPY NANOINDENTATION

Individual hair fibers from each sample were embedded in Epon 812 resin (TAAB Laboratories Equipment Ltd., Aldermaston, Berkshire, UK) by applying the mixed resin directly to the hair fibers, thereby avoiding infiltration of the resin into the sample. After curing, the resin blocks were mounted on steel atomic force microscopy (AFM) sample stubs with epoxy adhesive, and smooth axial and longitudinal sections of the hairs were obtained with an Ultracut N ultramicrotome (Reichert-Nissei, Tokyo, Japan) equipped with a diamond knife (Ultra 45, Diatome Ltd., Biel, Switzerland).

Nanoindentation experiments were performed with an MFP-3D scanning probe microscope (Asylum Research, Santa Barbara, California) equipped with a closed cell consisting of a reservoir situated around the sample mounting and a magnetically sealed rubber gasket attached to the head of the microscope. Various humidity conditions were achieved in the AFM cell through the use of saturated solutions of various chemicals, which were placed in the reservoir before the cell was sealed.

Details of the methods for calibrating the equipment for measurement and acquiring and evaluating the data are available elsewhere (3).

PROPERTIES OF THE MATRIX

MECHANICAL PROPERTIES

Electrostatic bonding within the matrix contributes additional structuring to that provided by the covalent cystine bonds of the crystalline keratin microfibrils. Consequently, the Young's modulus of hair in the dry state can be two to three times higher than that of the wet state. The degree of this contribution is inversely proportional to the hair's water content, which results in solvation of these temporary bonds. In short, wet-state tensile testing exclusively reflects the properties of the crystalline KIFs, whereas dry-state properties reflect additional contribution from the matrix.

Various hair insults have been widely reported to compromise hair's wet-state properties, but counterintuitively, such treatments often raise the dry-state Young's modulus. To illustrate this phenomenon, Figure 2A shows the decrease in wet modulus associated with bleaching treatments of increasing severity, whereas Figure 2B shows the dry-state modulus increasing for the same treatments. The plots in Figure 2C and D show similar increases in the dry modulus as a result of UV irradiation and exposure to the high temperatures associated with heat straightening, respectively.

Figure 2A indicates that the structural properties of the crystalline KIFs are compromised by these insults, so the increase of the dry-state modulus must constitute an increased matrix contribution. Moreover, in producing this dry-state increase, the enhanced matrix contribution must also overcome the often-sizable negatives associated with the degrading KIFs. For example, the approximately 10% increase in the dry-state modulus after a 9% bleaching treatment (Figure 2B) does not involve simply a 10% greater matrix contribution, but also involves mitigation of the 30% reduction in the contribution provided by the KIFs (Figure 2A).

In addition to the physical wetting of the fibers, hair's water content is determined by the relative humidity of the surrounding environment. Accordingly, hair's mechanical properties change in a systematic manner with variations in relative humidity (4). That is, rising relative humidity leads to increased water content and lesser mechanical properties. Therefore, if the wet-state modulus of bleached hair decreases but the dry-state modulus increases, then there must be a crossover point. Figure 3A shows the Young's modulus as calculated from tensile experiments as a function of relative humidity, whereas Figure 3B shows a comparable effect from torsion experiments.

Therefore, care is needed when reporting and contemplating hair's mechanical properties in that any experiment at a single set of conditions might represent a snapshot of a more complex scenario.

MODELING

The modeling of the viscoelastic properties of keratin fibers has been discussed by many researchers over the years. Classical models to describe this behavior have been suggested by Maxwell (5), Voigt (6), Eyring and coworkers (7–9), and others (10,11), and all involve the combination (parallel and/or serial arrangements) of springs and dashpots, where the springs represent the elastic component of the fibers (i.e., the crystalline phase, KIFs, in Figure 1) and the dashpots represent the viscous component (i.e., the amorphous phase,
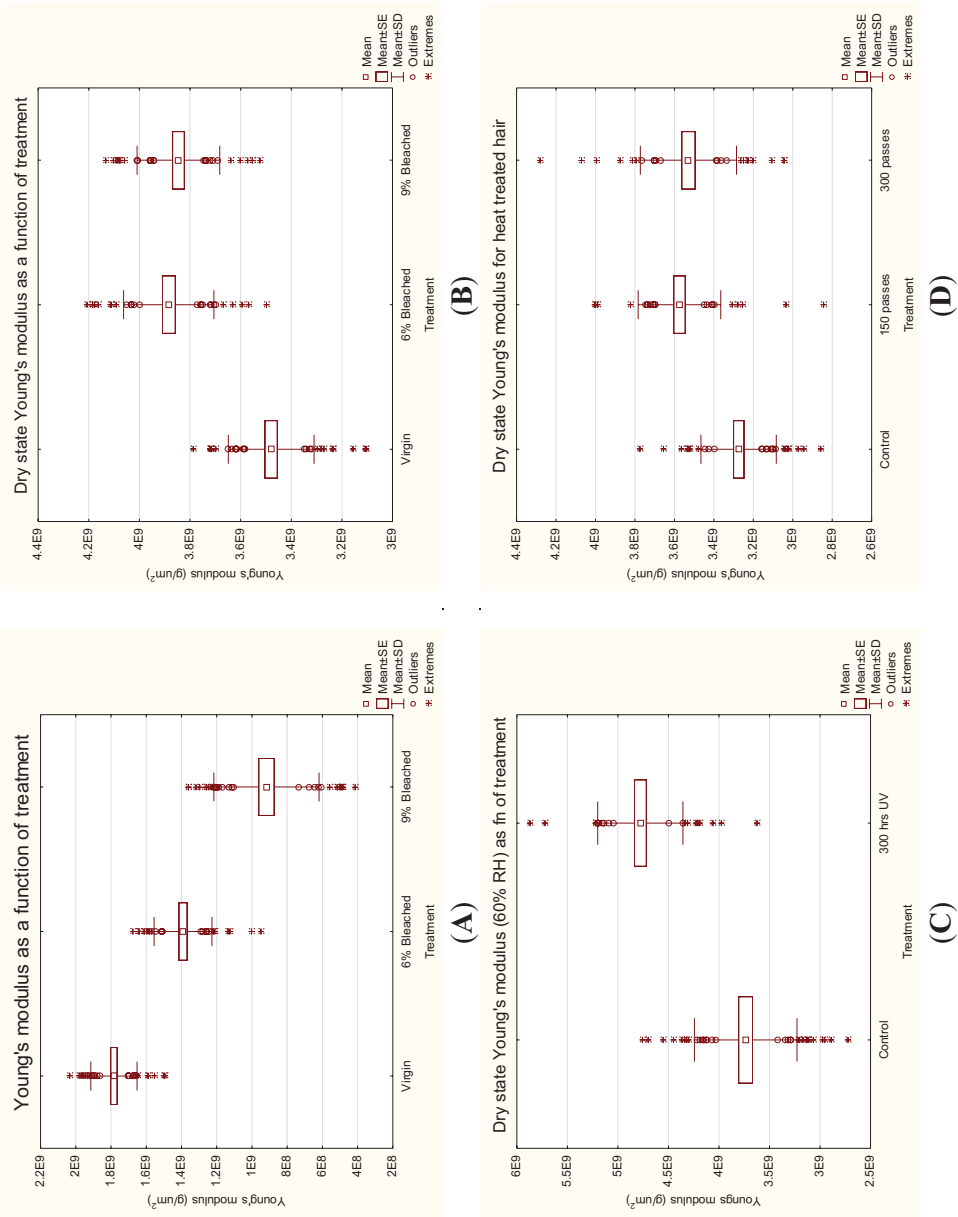
Figure 2. (A) Wet and (B) dry (60% RH) Young's moduli of virgin and oxidative-treated and (C,D) dry moduli of (C) UV- and (D) heat-treated hair fibers.
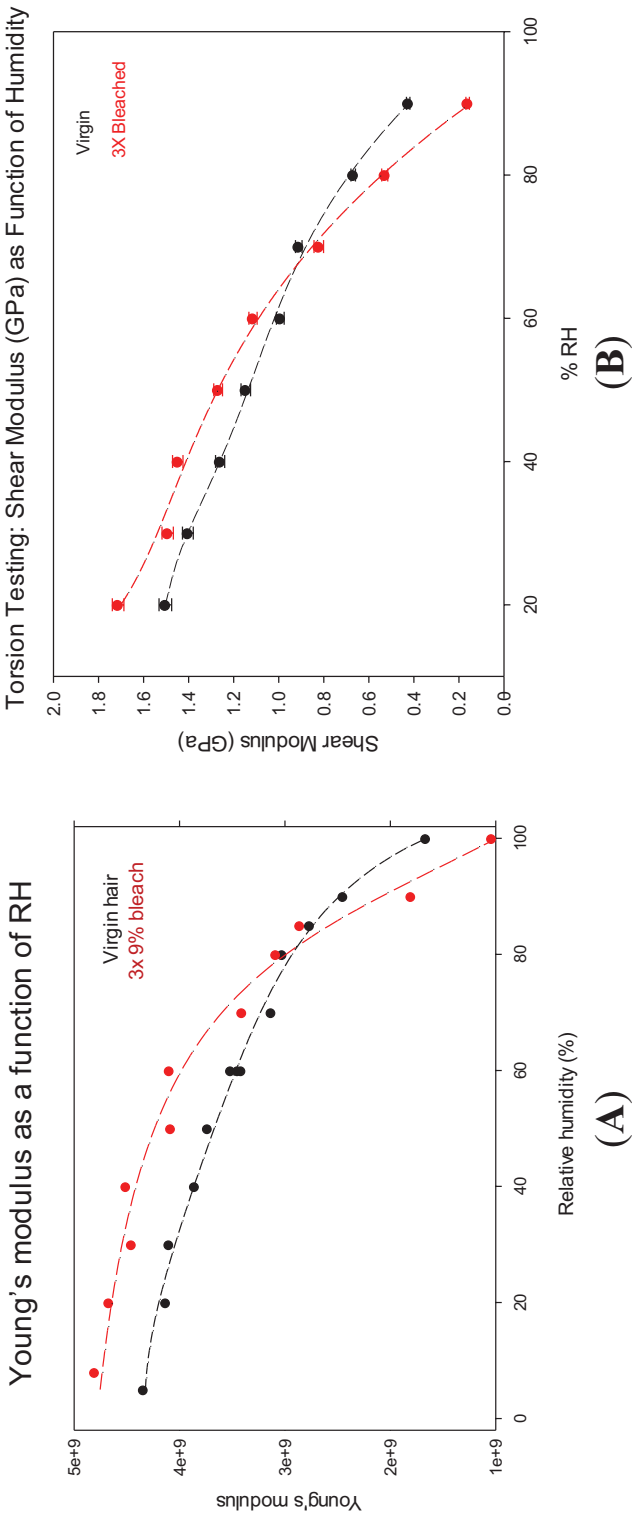
Figure 3. Influence of RH on hair's (A) extensional and (B) torsional moduli.

matrix, in Figure 1). The mathematical model describing the viscoelastic mechanics is given by the Kelvin–Voigt equation (6), which represents the fiber stress as the sum of the elastic (Hooke's law) and viscous (Newton's law) responses to the applied stress

$$\sigma(t) = E \cdot \varepsilon(t) + \eta \cdot \frac{d\varepsilon}{dt} \tag{1}$$

In Equation 1, $\sigma(t)$ represents the stress applied to the fiber during time t, $\varepsilon(t)$ is the recorded strain at the applied stress, E is the elastic modulus of the fiber, and η represents the viscosity of the material. An evaluation of the viscosity of keratin materials, for wool fibers at 20°C and 65% RH, produced values in the range of 10^{14}–10^{19} Pa, which suggests that the viscosity of the fibers, which is attributed to the matrix is at the limit of highly viscous fluids and soft solids (12).

Chemically, the crystalline phase (KIFs) is made of low-sulfur proteins, and the matrix consists of KAPs, classified as high-sulfur, ultrahigh-sulfur, and glycine–tyrosine-rich proteins (13).

For the modeling of the mechanics of hair, the matrix was considered to be a polymer cross-linked mainly by disulfide bonds and stabilized by a network of hydrogen bonds (14). The effect of the relative humidity on the fiber mechanics (see Figure 3A and B) is therefore understood as the result of water solvating the hydrogen bonds. One may assume, then, that the matrix behavior is strongly dependent on the abundance of electrostatic bonds and postulate that the complex Young's modulus of the fiber, E, is the sum of the contribution from the disulfide bonds, E_S, and that due to hydrogen bonds, E_H (15)

$$E = E_S + E_H \tag{2}$$

The contributions of the disulfide and hydrogen bonds to this complex modulus are proportional to the numbers of the respective bonds. For the case of hydrogen bonds, this proportionality is assumed to follow Nissan's model (16)

$$E_H = k_N N^{1/3} \tag{3}$$

where N is the number of effective hydrogen bonds per unit volume of keratin fibers and k_N is the constant of proportionality in Nissan's model.

An increase in relative humidity leads to a higher water content, which breaks hydrogen bonds and decreases the contribution of the second term, E_H, to the overall complex Young's modulus. This can be seen experimentally in Figure 3A and B. At 100% RH, the contribution of hydrogen bonds to the Young's modulus is nil, and the mechanics of the fiber are a reflection of only the disulfide bridges

$$E_{100\%RH} = E_S \tag{4}$$

These disulfide bonds can be cleaved by chemical treatments, such as oxidative bleaching, to form cysteic acid. In accordance with Equation 4, this should result in a decrease of the elastic modulus of the fiber when measured at 100% RH (see Figure 2A). The magnitude

of this effect will be proportional to the severity of the treatment and the resulting number of cleaved disulfide bonds.

Although tensile measurements provide some hints to the matrix chemistry and how the balance of the different bonds contribute to its mechanics, deeper investigation of the matrix requires other approaches. An especially precise alternative involves the use of AFM. This technique allows for the evaluation of the mechanical properties of the matrix with superior resolution, limited only by the size of the indenter tip. When this technique was investigated for examining the matrix mechanics, it was noticed that performing indentation on cross sections could not distinguish the effect of matrix filling the space between KIFs. This is because the resolution of the measurement, about 50 nm, is larger than the mean space between KIFs, which is about 10 nm (17). To overcome this difficulty, an elegant solution was employed, whereby information was acquired on the matrix by performing indentation on the longitudinal sections of the fiber (18).

Figure 4 shows results obtained by using AFM to investigate the properties of bleached and virgin fibers by this approach. This figure emphasizes the importance of using longitudinal sections during examination. Whereas the modulus values extracted from indentation of the cross sections of bleached and virgin fibers are not very different, the data for the longitudinal sections show the effects of bleaching on fiber mechanics, especially at low RH.

The two-phase model (see Figure 1) suggests that hair fibers consist of a composite material of rods embedded in a matrix. This allows the equations of Voigt (19) and Reuss (20) to be used to describe the elastic moduli of composite materials at axial and transverse stresses of E_{Axial} and E_{Trans}, respectively, in terms of the contributions of the moduli of the rods, E_{KIF}, and the matrix, E_{Matrix}. In this way, the modulus of the matrix can be evaluated from the AFM measurements on cross sections and longitudinal sections as (3)

$$E_{\text{Matrix}} = E_{\text{Trans}} \frac{E_{\text{KIF}} - E_{\text{Axial}}}{E_{\text{KIF}} - E_{\text{Trans}}} \tag{5}$$

By using Equations 2–4, one can evaluate the modulus of the matrix from the contribution of the disulfide and hydrogen bonds for both virgin and bleached fibers as (3)

$$E_{\text{Virgin Matrix}} = k_{\text{N}}(1 - n \cdot \text{EWC})^{1/3} + E_{\text{S}} \tag{6}$$

and

$$E_{\text{Bleached Matrix}} = 4.0e^{-0.022\text{RH}} + k_{\text{N}}(1 - n \cdot \text{EWC})^{1/3} + E_{\text{S}}' \tag{7}$$

where n is the number of water molecules required to break a hydrogen bond; EWC is the equilibrium water content of the fiber, which depends on RH; and E_{S} and E_{S}' are the elastic contributions of disulfide bonds to the virgin fibers and after the breaking of some fibers by bleaching, respectively.

Based on the AFM measurements and Equations 6 and 7, the Young's modulus of virgin matrix at 0% RH was estimated to be about 1.8 GPa, and that of bleached matrix at 0% RH was estimated to be about 5.5 GPa (3). The difference is interpreted as being due to the
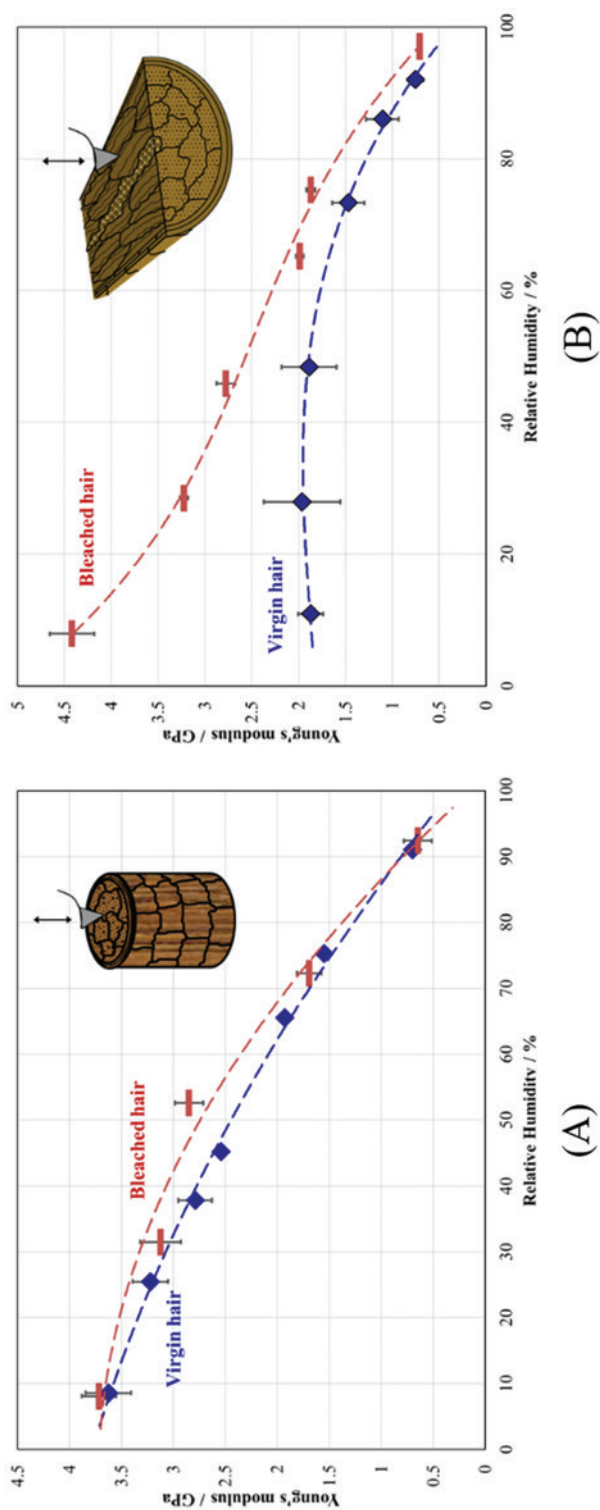
Figure 4. Elastic moduli of virgin and bleached fibers measured at various RH values on (A) Axial measurements (cross section) and (B) Transverse measurements (longitudinal section) of the fibers (18).

breaking of some disulfide bonds; the subsequent formation of cysteic acid; and a resulting increase in hydrogen bonding that stiffens the matrix, especially at low RH.

Equations 2 to 7 establish the physical background for evaluating the contribution of the matrix to the mechanical behavior of hair fibers (virgin and bleached) at different RH values and reflect the experimental results well (3).

DSC experiments also provide information on the nature of the matrix. Whereas the enthalpy of thermal denaturation (i.e., the area under the peak) is associated with the amount of α-helical protein contained within the fibers, the peak temperature, T_p, has been associated with the state of the matrix (see Figure 5) (21).

Two types of DSC experiments are commonly performed on keratin fibers. In the first, samples are placed in perforated capsules, and the hair is examined in the dry state (dry DSC). Alternatively, the samples can be sealed within high-pressure pans that also contain water (wet DSC) (22).

Results recorded in these two types of DSC experiments similarly exhibit differences in the detected responses to chemical treatments. Figure 6A shows results from wet-state DSC experiments where, as is commonly reported, the hair can be denatured at lower temperatures as a result of chemical bleaching. In contrast, Figure 6B shows that the dry-state denaturing temperature rises for these same samples.

This peak temperature is related to the state of the matrix (see Figure 5). In the wet state, this structure contributes a lesser stabilizing effect, and the KIFs denature at lower temperatures. However, the opposite situation arises in the dry state, which implies that the matrix becomes more rigid and contributes additional stabilization to the KIFs. These findings are consistent with the previously described observations for the mechanical properties (23).
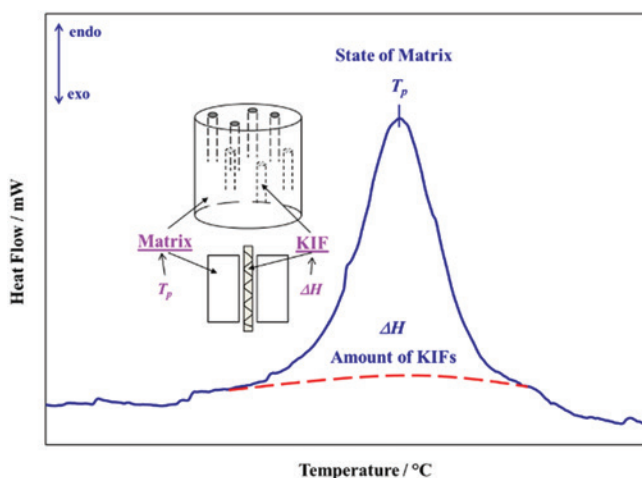

Figure 5. Relationship between the components of hair and DSC/differential thermal analysis (DTA) endothermal parameters (21).
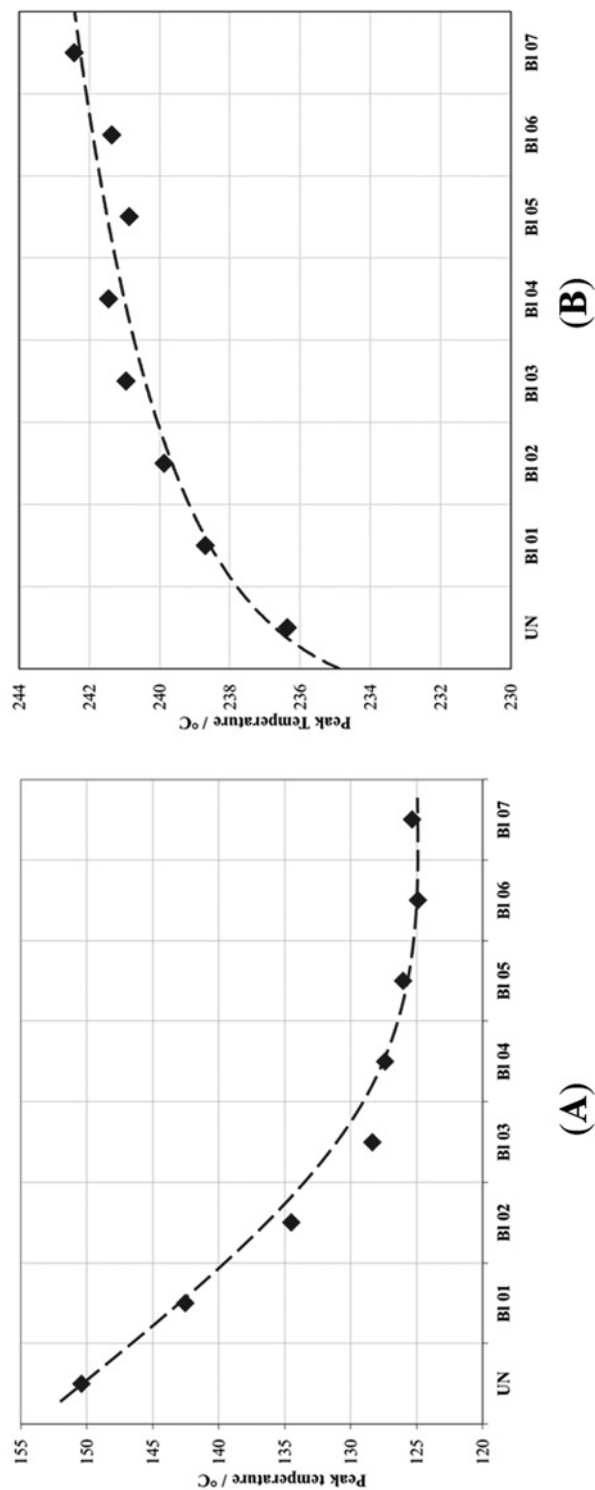
Figure 6. Influence of chemical treatments on the denaturing peak temperature for hair (T_p) as determined by (A) wet and (B) dry DSC.
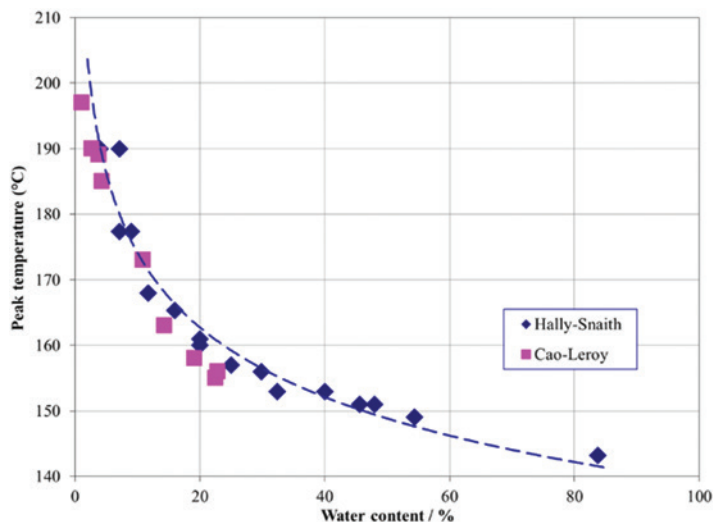
Figure 7. Evolution of the peak temperature of keratin fibers with increasing water content, as reported by Haly and Snaith for DTA measurements on wool (24) and by Cao and Leroy for DSC measurements on hair (25). The experimental points fit the WLF model (26), as shown by the dotted curve (27).

Yet, as before, wet and dry represent extremes, and previous DSC/DTA, experiments on wool (24) and hair (25) showed that the denaturing temperature decreases with progressively increasing water content as obtained by varying the relative humidity (see Figure 7). These experimental data appear to be well fit by the Williams–Landel–Ferry (WLF) model (26), given by the equation

$$\ln(a_{\text{T}}) = \frac{C_1(T - T_{\text{Reference}})}{C_2 + T - T_{\text{Reference}}} \tag{8}$$

where a_{T} reflects primarily the temperature dependence of a segmental friction coefficient or mobility on which the rates of all configurational rearrangements depend, C_1 and C_2 are empirical constants, and $T_{\text{Reference}}$ is 50°C. This fit allows for the conclusion that the matrix is a viscous material (27), corresponding to the viscous component of the viscoelastic description of the mechanical behavior of hair given by Equation 1.

STRUCTURE AND MORPHOLOGY OF THE MATRIX

Historically, the matrix has generally been viewed as an amorphous, cross-linked polymer, but the fine details of its structure were less investigated. The relatively recent progress in the analysis of KAP structures (10) has rekindled interest in studying the matrix morphology.

Some of the early proposals for the fine structure of the matrix were based on an analysis of tensile measurements on wool. Crewther suggested that a layer of matrix molecules protects the helical structure of the microfibrils (28). In a second work on the same topic,
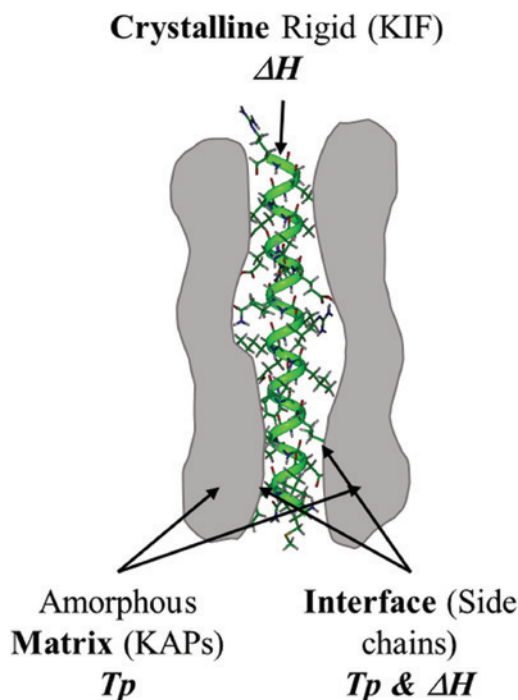
Figure 8. Three-phase model and DSC measurements that reflect the states of the model's three components (22,31–33).

Crewther stated that there is an "essentially uniform interaction between the microfibrils and the high-sulfur proteins of the matrix" (29). Chapman came to a similar conclusion regarding disulfide links between a less-ordered matrix and the KIFs (30).

These works suggest that there is an interface between the matrix and the KIFs. In other words, it appears that the two-phase model (see Figure 1) needs to be upgraded to include three phases. Solid-state nuclear magnetic resonance (NMR) experiments involving hair, as well as DSC studies on hair at different pH values, also suggest that a three-phase model for hair (shown in Figure 8) could better explain the properties of hair (31,32).

Assuming the existence of an interface between the matrix and the KIFs also necessitates adjustments to the meanings of peak temperature and enthalpy, particularly for the values recorded from the wet DSC of hair, from those given in Figure 5 to a more complex picture, suggested in Figure 8 (22,33).

Crewther also suggested that the protein globules (KAPs) of the matrix, which contain a large number of internal disulfide cross-links, covalently linked to each other to form a "loose, randomly arranged or only partly oriented, network of beaded chains" (29). This model of a beaded matrix is further supported by solid-state NMR data (34), and as depicted in Figure 9, it explains well the effects of the bleaching process (18,34).

Recent experiments measuring the transport of heat through hair fibers by a transient electrothermal (TET) technique (35) also suggested a grainy nanoscale matrix structure,
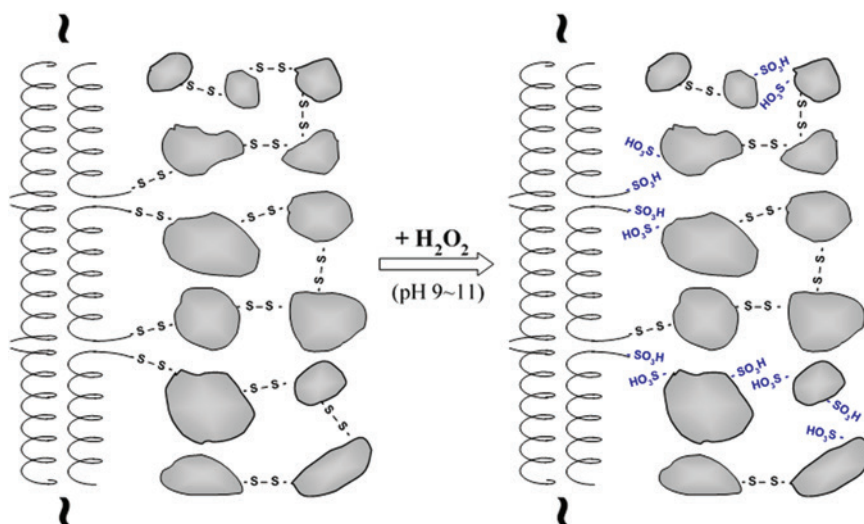
Figure 9. Matrix beaded-chain model describing the effects of the bleaching process on hair (18,34)

which is in line with the idea of globular KAPs in the matrix, in accordance with the models proposed by Crewther (29) and later by Feughelman (36) and critically summarized by Hearle (37). The model of the matrix supported by these results is similar to the original beaded model of Crewther (29). Moreover, the TET results indicate that the grains exhibit a certain order at the nanoscale, which implies organization of the proteins and not a random packing of chains associated with densely cross-linked disulfide bonds (35).

The model of hair given in Figure 10 summarizes these results and suggests that there is, still, more to investigate concerning the structure of matrix.
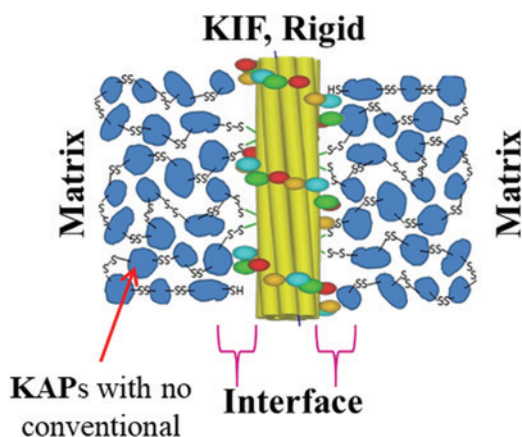

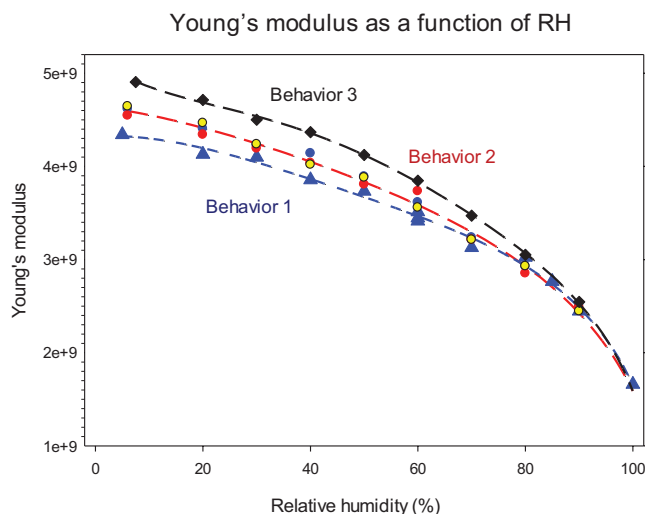**Figure 10.** Hair model with a grainy matrix (38).

Figure 11. Differing shapes for Young's moduli versus RH curves for single-source hairs obtained from different individuals.

CONCLUSION

The work reported herein attempts to demonstrate how experiments performed in the wet state yield only part of the story regarding hair's physical properties. Specifically, such experiments contain no contribution from the amorphous KAPs, that is, the matrix. Yet, this structure can be the dominant contributor to certain properties, such as fiber stiffness. Furthermore, the results from dry-state experiments, which do include matrix contributions, can produce outcomes contrary to well-established beliefs. For example, damaging chemical treatments can raise hair's dry-state modulus and produce higher dry-state protein denaturing temperatures.

Approaches have been described for modeling the contributions of the various internal structures to hair properties, while similarly incorporating the sizable effects of water content. To this end, experiments at low humidity (i.e., low water content) contain higher contributions from the innate matrix structure, for which the disruptive effects of moisture are minimized. Testing is rarely performed under these conditions, and new insights may be waiting in experiments performed under these conditions. For example, Figure 11 shows results from modulus versus humidity experiments that were performed on different hair samples obtained from a variety of individual donors. These curves superimpose and suggest no differences at high water content, but considerable divergence occurs at low humidity.

The properties of hairs obtained from individual heads can be substantially altered by habits and practices; yet, all of our donors reported no use of chemical treatments. Moreover, the three behaviors shown in Figure 11 were repeatedly encountered, whereas more random outcomes would presumably be expected if the hairs exhibited substantial contributions from the diversity of consumer practices.

In accordance with the principles outlined herein, these mechanical properties imply differences in the internal structures of the hairs from these individuals—particularly in the structure and morphology of the amorphous matrix. This presumption is outside the

limits of conventional thinking with regard to hair structure, but perhaps there are some accepted ideas within the literature that might provide an explanation.

Specifically, the existence of different types of cortical cells containing differing quantities of matrix protein has been reported (39). Conceptually, then, a higher proportion of high-sulfur cortical cells would presumably enhance dry-state mechanics while perhaps impacting other related properties, such as diffusion rates into hair fibers. The pursuit of these nonstandard ideas will be the subject of future research activities.

REFERENCES

(1) M. Feughelman, A two-phase structure for keratin fibers, *Text. Res. J.*, **29**(3), 223–228 (1959).

(2) D. Persaud and Y. K. Kameth, Torsional method for evaluating hair damage and performance of hair care ingredients, *J. Cosmet. Sci.*, **55**(Suppl), S65–S77 (2004).

(3) S. Breakspear, B. Noecker, and C. Popescu, Relevance and evaluation of hydrogen and disulfide bond contribution to the mechanics of hard α-keratin fibers, *J. Phys. Chem. B*, **123**(21), 4505−4511 (2019).

(4) C. Popescu and H. Höcker, Chapter 4. Cytomechanics of hair. Basics of the mechanical stability, *Int. Rev. Cell Mol. Biol.*, **277**(C), 137–156 (2009).

(5) J. C. Maxwell, The Bakerian Lecture. On the viscosity or internal friction of air and other gases, *Philos. Trans. R. Soc. London*, **156**, 249–268 (1866).

(6) W. Voigt, *Kompendium der theoretischen Physik, Band I* (De Gruyter, Leipzig, Germany, 1895).

(7) A. Tobolsky and H. Eyring, Mechanical properties of polymeric materials. *J. Chem. Phys.*, **11**, 125–135 (1943).

(8) G. Halsey, H. J. White, Jr., and H. Eyring, Mechanical properties of textiles, I, *Text. Res. J.*, **15**(9), 295–311 (1945).

(9) C. E. Reese and H. Eyring, Mechanical properties and the structure of hair, *Text. Res. J.*, **20**(11), 743–753 (1950).

(10) L. Peters and J. B. Speakman, The visco-elastic properties of wool fibers, *Text. Res. J.*, **18**(9), 511–518 (1948).

(11) M. Feughelman, Natural protein fibers, *J. Appl. Polym. Sci.*, **83**(3), 489–507 (2002).

(12) F.-J. Wortmann and S. De Jong, Nonlinear viscoelastic behavior of wool fibers in a single step relaxation test. *J. Appl. Polym. Sci.*, **30**(5), 2195–2206 (1985).

(13) R. D. B. Fraser and D. A. D. Parry, "Trichocyte keratin-associated proteins (KAPs)", in *The Hair Fibre: Proteins, Structure and Development*, J. E. Plowman, D. Harland, and S. Deb-Choudhury, Eds. (Springer Nature Singapore Pty Ltd., Singapore, 2018), pp. 71–86. Advances in Experimental Medicine and Biology, vol. 1054.

(14) T. W. Mitchell and M. Feughelman, The torsional properties of single wool fibers. Part I: Torque-twist relationships and torsional relaxation in wet and dry fibers. *Text. Res. J.*, **30**(9), 662–667, (1960).

(15) C. Popescu, Mechanomics, Princeton, New Jersey, September 18–19 2014. 6th International Conference on Applied Hair Science: TRI Princeton.

(16) A. H. Nissan, H-bond dissociation in hydrogen bond dominated solids. *Macromolecules*, **9**(5), 840–850 (1976).

(17.) Y. Kajiura, S. Watanabe, T. Itou, K. Nakamura, A. Iida, K. Inoue, N. Yagi, Y. Shinohara, and Y. Amemiya, Structural analysis of human hair single fibres by scanning microbeam SAXS. *J. Struct. Biol.*, **155**(3), 438–444 (2006).

(18) S. Breakspear, The Contribution of Non-Covalent Strategic Bonds to the Nanomechanical Properties of Hair, Redbank, New Jersey, June 8–9 2016, 7th International Conference on Applied Hair Science: TRI Princeton.

(19) W. Voigt, Ueber die Beziehung zwischen den beiden Elasticitätsconstanten isotroper Körper, *Ann. Phys.*, **274**(12), 573–587 (1889).

(20) A. Reuss, Berechnung der Fließgrenze von Mischkristallen auf Grund der Plastizitätsbedingung für Einkristalle. *Z. Angew. Math. Mech.*, **9**(1), 49–58 (1929).

(21) C. Popescu and F.-J. Wortmann, HPDSC evaluation of cosmetic treated human hair, *Rev. Roum. Chim.*, **48**(12), 981–986 (2003).

(22) C. Popescu and C. Gummer, DSC of human hair: a tool for claim support or incorrect data analysis? *Int. J. Cosmet. Sci.*, **38**(5), 433–439 (2016).

(23) F.-J. Wortmann, G. Wortmann, and C. Popescu, Linear and nonlinear relations between DSC parameters and elastic moduli for chemically and thermally treated human hair, *J. Therm. Anal. Calorim.*, **140**, 2171–2178 (2020).

(24) A. R. Haly and J. W. Snaith, Differential thermal analysis of wool–the phase-transition endotherm under various conditions, *Text. Res. J.*, **37**(10), 898–907 (1967).

(25) J. Cao and F. Leroy, Depression of the melting temperature by moisture for alpha-form crystallites in human hair keratin, *Biopolymers*, **77**(1), 38–43 (2005).

(26) M. L. Williams, R. F. Landel, and J. D. Ferry, The temperature dependence of relaxation mechanisms in amorphous polymers and other glass-forming liquids, *J. Am. Chem. Soc.*, **77**(14), 3701–3707 (1955).

(27) C. Popescu and F.-J. Wortmann, The Behaviour of Keratins at High Temperature, Krakow, Poland, 27–31 Aug 2006, 9th European Symposium on Thermal Analysis and Calorimetry: Polish Society of Thermal Analysis and Calorimetry.

(28) W. G. Crewther, The stress–strain characteristics of animal fibers after reduction and alkylation, *Text. Res. J.*, **35**(10), 867–877 (1965).

(29) W. G. Crewther, The effects of disaggregating agents on the stress–strain relationship for wool fibers, *Text. Res. J.*, **42**(2), 77–85 (1972).

(30) B. M. Chapman, A mechanical model for wool and other keratin fibers, *Text. Res. J.*, **39**(12), 1102–1109 (1969).

(31) M. Baias, D. E. Demco, C. Popescu, R. Fechete, C. Melian, B. Blümich, and M. Möller, Thermal denaturation of hydrated wool keratin by ^{1}H solid-state NMR, *J. Phys. Chem. B*, **113**(7), 2184–2192 (2009).

(32) D. Istrate, C. Popescu, M. Er Rafik, and M. Möller, The effect of pH on the thermal stability of fibrous hard alpha-keratins, *Polym. Degrad. Stab.*, **98**(2), 542–549 (2013).

(33) D. Istrate, C. Popescu, and M. Möller, Nonisothermal kinetics of hard α-keratin thermal denaturation, *Macromol. Biosci.*, **9**(8), 805–812 (2009).

(34) M. Baias, D. E. Demco, D. Istrate, C. Popescu, B. Blümich, and M. Möller, Morphology and molecular mobility of fibrous hard α-keratins by ^{1}H, ^{13}C, and ^{129}Xe NMR, *J. Phys. Chem. B*, **113**(35), 12136–12147 (2009).

(35) M. Kadir, X. Wang, B. Zhu, J. Liu, D. Harland, and C. Popescu, The structure of the "amorphous" matrix of keratins, *J. Struct. Biol.*, **198**(2), 116–123 (2017).

(36) M. Feughelman, A model for the mechanical properties of the α-keratin cortex, *Text. Res. J.*, **64**(4), 236–239 (1994).

(37) J. W. S. Hearle, A critical review of the structural mechanics of wool and hair fibres, *Int. J. Biol. Macromol.*, **27**(2), 123–138 (2000).

(38) M. Kadir, Phonon and Spin Diffusion in Single Hair Fiber: Structure of the Amorphous Matrix of Keratins, Redbank, New Jersey, June 8–9 2016, 7th International Conference on Applied Hair Science: TRI Princeton.

(39) D. Harland, Hair's multi-scalar architecture, Redbank, New Jersey, June 8–9 2016, 7th International Conference on Applied Hair Science: TRI Princeton.